The Simple Yet Elusive Crystal Structure of Silver Acetate and the Role of the Ag−Ag Bond in the Formation of Silver Nanoparticles during the Thermally Induced Reduction of Silver Carboxylates

Leif P. Olson,*,† David R. Whitcomb,‡ Manju Rajeswaran,† Thomas N. Blanton,† and Barbara J. Stwertka†

Eastman Kodak Company, 1669 Lake Avenue, Rochester, New York 14650-2158, and Eastman Kodak Company, 1 Imation Way, Oakdale, Minnesota 55129

Received December 1, 2005. Revised Manuscript Received January 18, 2006

We report the single-crystal X-ray structure of silver acetate, accompanied by Raman spectra and density functional theory calculations. This work should aid understanding of the process of forming silver nanoparticles during the thermally induced reduction of silver carboxylates, e.g., in thermographic materials. The structure of silver acetate comprises the often-observed $Ag_2(carboxylate)_2$ dimer unit connected by interdimer Ag−O bonds to form infinite chains that align in a parallel fashion, forming stacks. The presence in the dimer of a Ag−Ag bond via closed-shell $d^{10}-d^{10}$ interactions is determined by Atoms in Molecules methodology, tentatively supported by the experimental observation of Raman scattering peaks (also found by vibrational frequency calculations) for Ag−Ag stretching. The Ag(I)−Ag(I) bond may be an important precursor to metallic silver formation, as single-electron reduction of the $Ag_2(carboxylate)_2$ species could result in the formation of $(Ag_2)^{+\bullet}$, known in photographic chemistry as a precursor to metallic silver clusters. The calculated structure of the radical anion of silver acetate consists of a $(Ag_2)^{+\bullet}$ cluster complexed by two acetate ions, lending support to earlier postulates that Ag−Ag bonding may promote the formation of silver nanoparticles during the thermally induced reduction of silver carboxylates.

Introduction

Silver carboxylates have been used in photothermographic (PTG) imaging materials as the source of silver for the formation of metallic silver nanoparticles, which comprise the image, since commercial photothermographic materials became available in 1964.[1] In these materials, the silver ion is reduced with an organic reducing agent, typically phenolic-based structures, simply by heating to a specific temperature, typically around 120 °C or higher. The mechanism by which the development reaction occurs is only partially understood,[1,2] but it is clear that the class of silver carboxylates is particularly useful and, in fact, is virtually the only silver source used today. Of particular interest for photothermographic materials are the long-chain versions, such as silver stearate and silver behenate, having 18 and 22 carbons in the hydrocarbon chain, respectively. Formally speaking, the compounds are actually bis-silver octadecanoate, $[Ag(O_2C_{18}H_{35})]_2$, and bis-silver docosanoate, $[Ag(O_2C_{22}H_{45})]_2$, by virtue of the fact that the molecules consist of dimeric pairs of silver bridged by the carboxylate ligand, Figure 1.

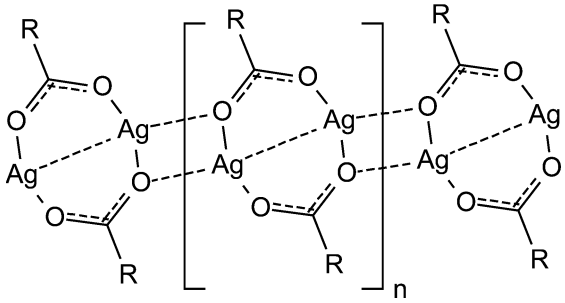

Figure 1. Silver carboxylate dimer.

In addition to the fact that the "eight-membered ring" dimer building block is virtually universally observed in all simple silver carboxylate structures, including silver stearate[3a] and silver trifluoroacetate,[3b] one of the most interesting features of that dimer is that the Ag−Ag separation is commonly within the normal bonding distance of metallic silver, 2.889 Å. Such a close Ag(I)−Ag(I) contact is interesting, as the singly occupied 5s orbital of Ag(0) is expected to participate in Ag−Ag bonding but is vacant in Ag(I), so there is no unpaired electron to share. In such a case, coulombic repulsion would normally be expected to prevent close association of the two positively charged ions, despite some relief of the full positive charges by overlap with electron-donating species, such as negatively charged

* To whom correspondence should be addressed. E-mail: leif.olson@kodak.com.Tel: 585-477-0928. Fax: 585-588-7611.
† Eastman Kodak Company, Rochester, New York.
‡ Eastman Kodak Company, Oakdale, Minnesota.

(1) Cowdery-Corvan, J. P.; Whitcomb, D. R. In *Handbook of Imaging Materials*; Diamond, A. S., Weiss, D. S., Eds.; Marcel-Dekker: New York, 2002. (b) Whitcomb, D. R. *Kirk Othmer Encyclopedia of Chemical Technology*; John Wiley & Sons: New York, 2003; online edition.
(2) Sahyun, M. R. V. *J. Imaging Sci. Technol.* **1998**, *42*, 23.
(3) (a) Tolochko, B. P.; Chernov, S. G.; Nikitenko, S. G.; Whitcomb, D. R. *Nucl. Instrum. Methods Phys. Res., Sect. A* **1998**, *405*, 428. (b) Griffin, R. G.; Ellett, J. D.; Mehring, M.; Bullitt, J. G.; Waugh, J. S. *J. Chem. Phys.* **1972**, *57*, 2147.

10.1021/cm052657v CCC: $33.50
Published on Web 02/15/2006

ligands. Many complexes of Ag(I) with various types of ligands (some quite different than carboxylate) display similarly close Ag(I)−Ag(I) interactions, commonly enough that this phenomenon has been named argentophilicity.[4] Although the parallel concept and firmly established phenomenon of aurophilicity (for Au(I) complexes) is widely accepted as a genuine bonding situation, in the case of Ag(I), there has been less unanimity as to whether this is an attractive interaction (i.e., bonding) or whether there is a net repulsion that is, in most cases, counteracted by the bidentate structure of the ligand holding the two silver ions in proximity. Literature reports, including both computational and structural studies that discuss the possibility of a silver−silver bond in silver carboxylate structures, have been divided into bonding and nonbonding camps.[5] The observation of completely ligand-unsupported Ag(1)−Ag(1) interactions[4c,5m] seems to settle the issue in favor of argentophilicity as a real phenomenon; nonetheless, it does not prove that a given ligand-supported Ag−Ag interaction is argentophilic, and therefore additional study of this topic is warranted.

The process of adding an electron, such as during the initial stage of thermal or photochemical decomposition of the silver carboxylate, has been suggested[2,6] as a means for generating $(Ag_2)^{+\bullet}$, which is considered by some photographic theories to be the minimal stable latent image center in silver halides.[7] If the analogous monocation dimer were formed in the silver carboxylate salt in the PTG system, established techniques from photographic science might be utilized to better control the formation of metallic silver nanoparticles as well as the development process in these systems.

We have undertaken the task of extending our investigation of silver compounds to probing the solid-state structure and computationally modeled silver carboxylates with a dimeric structure but a size that can readily be computationally accessed, such as silver acetate, to provide a better understanding of the development process of photothermographic imaging materials. As a continuation of our work to elucidate the structures of silver carboxylate complexes important to PTG technology,[3a,8] we report here the solid-state structure of silver acetate, surprisingly not previously published (to the best of our knowledge) despite its simplicity, even though the structure of silver trifluoroacetate (AgO_2CCF_3) was published[3b] more than 30 years ago. Presumably, it has proven elusive because of the difficulty in obtaining good quality crystals and because of the difficulty in indexing in this case. The low-frequency (from 400 cm^{-1} to approximately 70 cm^{-1}) Raman spectra of silver acetate with 633 and 785 nm excitation are reported as well. In addition, we report theoretical studies of the electronic structures of $Ag_2(O_2C_2H_3)_2$ and $[Ag_2(O_2C_2H_3)_2]_3$ as models for the larger silver carboxylates used in PTG imaging. This was done primarily using density functional theory (DFT) calculations[9] for geometry optimizations and computation of vibrational frequencies and the atoms in molecules theory[10] for evaluating the topology of the DFT-computed electron density. The computational results help explain how the silver carboxylate dimer structure contributes to the overall imaging properties observed in PTG imaging materials.

Experimental Procedures

Silver Acetate Preparation. Silver acetate was obtained from Aldrich Chemical Co. and recrystallized from the slow cooling of a filtered (1.6 μ glass fiber) warm water solution containing 1 mol % (relative to silver) acetic acid. The crystals were of adequate size for single-crystal XRD analysis; however, defects were visible, indicating that the quality of the crystals could impact the overall quality of the single-crystal data. Nonetheless, these single crystals were sufficient for successful single-crystal structure determination.

Crystal Structure Determination. A colorless, thin, long, needle-shaped crystal of silver acetate with approximate dimensions $0.02 \times 0.04 \times 0.75$ mm^3 was chosen for data collection. All attempts to cut these needles into shorter lengths were unsuccessful because of lengthwise shearing (breaking into thin fibers). Diffraction data were collected at room temperature using a Nonius Kappa-CCD diffractometer with graphite-monochromated Mo Kα radiation ($\lambda = 0.71073$ Å). A total of 391 frames were collected using $\varphi + \omega$ scans to fill the asymmetric unit with a scan range of 1.3° and a counting time of 45 s per frame. The first 10 frames were used for indexing reflections using the *DENZO*[11] software package and

(4) (a) Wang, Q.; Mak, T. C. W. *J. Am. Chem. Soc*. **2001**, *123*, 7594. (b) Guo-Cong, G.; Mak, T. C. W. *Angew. Chem., Int. Ed.* **1998**, *38*, 262. (c) Omary, M. A.; Webb, T. R.; Assefa, Z.; Shankle, G. E.; Patterson, H. H. *Inorg. Chem*. **1998**, *37*, 1380.

(5) (a) Pyykkö, P. *Chem. Rev*. **1997**, *97*, 597. (b) Cotton, F. A.; Feng, X.; Matusz, M.; Poli, R. *J. Am. Chem. Soc.* **1988**, *110*, 7077. (c) Pyykkö, P.; Runeberg, N.; Mendizabal, F. *Chem.—Eur. J.* **1997**, *3*, 1451. (d) Pyykkö, P.; Mendizabal, F. *Chem.—Eur. J.* **1997**, *3*, 1458. (e) Fernández, E.; Lopez-de-Luzuriaga, J. M.; Monge, M.; Rodríguez, M. A.; Crespo, O.; Gimeno, M. C.; Laguna, A.; Jones, P. G. *Inorg. Chem*. **1998**, *37*, 6002. (f) El-Bahraoui, J.; Molina, J. M.; Olea, D. P. *J. Phys. Chem. A* **1998**, *102*, 2443. (g) Runeberg, N.; Schütz, M.; Werner, H.-J. *Chem. Phys*. **1999**, *110*, 7210. (h) Hermann, H. L.; Boche, G.; Schwerdtfeger, P. *Chem.—Eur. J*. **2001**, *7*, 5333. (i) Jiang, Y.; Alvarez, S.; Hoffmann, R. *Inorg. Chem*. **1985**, *24*, 749. (j) Mehrotra, P. K.; Hoffmann, R. *Inorg. Chem.* **1978**, *17*, 2187. (k) Merz, K. M.; Hoffmann, R. *Inorg. Chem*. **1988**, *27*, 2120 and references therein. (l) Michaelides, A.; Skoulika, S.; Kiritsis, V.; Aubre, A. *Chem. Commun*. **1995**, 1415. (m) Singh, K.; Long, J. R.; Stavropoulos, P. *J. Am. Chem. Soc.* **1997**, *119*, 2942. (n) Kristiansson, O. *Inorg. Chem*. **2001**, *40*, 5058. (o) A good summary is provided in: Sailaja, S.; Rajasekharan, M. V. *Inorg. Chem*. **2003**, *42*, 5675.

(6) Bokhonov, B.; Burleeva, L.; Usanov, Y.; Whitcomb, D. R. *J. Imaging Sci. Technol*. **2001**, *45*, 259.

(7) (a) Hamilton, J. F. The mechanism of formation of the latent image. In *The Theory of the Photographic Process*, 4th ed.; James, T. H., Ed.; Eastman Kodak Company: Rochester, NY, 1977; Chapter 4. (b) Carroll, B. H. The mechanism of latent image formation. In *Introduction to Photographic Theory*; Carroll, B. H., Higgins, G. C., James, T. H., Eds.; Wiley-Interscience: New York, 1980; Chapter 7.

(8) Whitcomb, D. R.; Rajeswaran, M. *J. Imaging Sci. Technol*. **2003**, *47*, 107. (b) Whitcomb, D. R.; Rogers, R. D. *J. Imaging Sci. Technol*. **1999**, *43*, 504. (c) Whitcomb, D. R.; Rogers, R. D. *Polyhedron* **1997**, *16*, 863. (d) Whitcomb, D. R.; Rogers, R. D. *Inorg. Chim. Acta* **1997**, *256*, 263. (e) Whitcomb, D. R.; Rogers, R. D. *J. Chem. Cryst*. **1996**, *26*, 99. (f) Whitcomb, D. R.; Rogers, R. D. *J. Chem. Crystallogr*. **1995**, *25*, 137.

(9) Becke, A. D. *J. Chem. Phys*. **1993**, *98*, 5648. (b) Becke, A. D. *Phys. Rev. A*. **1988**, *38*, 3098. (c) Lee, C.; Yang, W.; Parr, R. G. *Phys. Rev. B* **1988**, *37*, 785. (d) Miehlich, B.; Savin, A.; Stoll, H.; Preuss, H. *Chem. Phys. Lett*. **1989**, *157*, 200.

(10) Bader, R. F. W. *Atoms In Molecules: A Quantum Theory*; Oxford University Press: Oxford, UK, 1990. (b) Cioslowski, J.; Hanayakkara, A.; Challacombe, M. *Chem. Phys. Lett*. **1993**, *203*, 137. (c) Cioslowski, J.; Surjan, P. R. *J. Mol. Struct*. **1992**, *9*, 255. (d) Stefanov, B. B.; Cioslowski, J. *J. Comput. Chem*. **1995**, *16*, 1394. (e) Cioslowski, J. *Int. J. Quantum Chem., Quantum Chem. Symp*. **1990**, *24*, 15. (f) Cioslowski, J.; Mixon, S. T. *J. Am. Chem. Soc*. **1991**, *113*, 4142. (g) Cioslowski, J. *Chem. Phys. Lett*. **1992**, *194*, 73. (h) Cioslowski, J. *Chem. Phys. Lett*. **1994**, *219*, 151.

(11) *DENZO*: Otwinowski, Z.; Minor, W. *Methods in Enzymology, Vol. 276*: *Macromolecular Crystallography, part A*; Carter, C. W., Jr., Sweet, R. M., Ed.; Academic Press: New York, 1997; pp 307−326.

Table 1. Crystal Data and Structure Refinement for Silver Acetate, $[Ag(O_2CCH_3)]_2$

empirical formula	$C_{14}H_{21}Ag_7O_{14}$
fw	1168.40
T (K)	293(2)
wavelength (Å)	0.71073
cryst syst	triclinic
space group	$P\bar{1}$
a (Å)	5.5810(11)
b (Å)	9.960(2)
c (Å)	21.587(4)
α (deg)	89.10(3)
β (deg)	97.40(3)
γ (deg)	97.26(3)
V (Å^3)	1180.4(4)
Z	2
D_{calcd} (Mg/m^3)	3.287
abs coeff (mm^{-1})	5.752
F(000)	1092
cryst size (mm^3)	0.02 × 0.04 × 0.75
θ range for data collection (deg)	1.90−26.86
index ranges	$-7 \le h \le 5$, $-12 \le k \le 12$, $-27 \le l \le 27$
no. of reflns collected	7662
no. of independent reflns	4784 [R(int) = 0.0989]
completeness to $\theta = 26.86°$ (%)	94.2
abs corr	none
refinement method	full-matrix least-squares on F^2
data/restraints/params	4784/0/183
GOF on F^2	0.892
final R indices [$I > 2\sigma(I)$]	R1 = 0.0711, wR2 = 0.1373
R indices (all data)	R1 = 0.2536, wR2 = 0.2029
largest diff. peak and hole (e Å^{-3})	1.729 and −1.691

were refined to obtain final cell parameters. Data reductions were performed using *DENZO−SMN*.[11] A total of 7662 reflections had their intensities integrated and scaled, of which 4784 reflections were independent with a quite high R_{merg} value of 0.099, and 1474 reflections were above $4\sigma(I)$. A numerical absorption correction applied by the *SORTAV*[12] program was found to be insignificant. The unit cell for silver acetate was determined to be triclinic, space group $P\bar{1}$, with unit cell dimensions of a = 5.5810 (11) Å, b = 9.960 (2) Å, c = 21.587 (4) Å, α = 89.10(3)°, β = 97.40(3)°, and γ = 97.26(3)°. We collected multiple reflection data sets but were successful in structure determination using this particular data set. For most of the unsuccessful data sets, one of the unit cell indices was double or triple the value of the correct unit cell indices. The initial solution for this structure was obtained by direct methods using *SHELXTL*;[13] the remaining carbon atoms were found by successive cycles of least-squares refinements followed by electron-density maps. The structure was refined by full-matrix least-squares on F^2 with anisotropic displacement parameters for Ag atoms only using *SHELXTL*. The remaining non-hydrogen atoms were left isotropic because of a very low ratio of observable reflections to total number of independent reflections. Before the final least-squares cycles, hydrogen atoms were placed in idealized positions and refined as riding atoms with isotropic displacement parameters. The structure refined to a goodness of fit (GOF) of 0.892 and final residuals of R1 = 0.0711% ($I > 2\sigma(I)$), wR2 = 0.1373% ($I > 2\sigma(I)$). The relatively high R value and low data-to-parameter ratio is related to the weak diffraction and poor crystal quality. Details of the crystallography and crystal parameters are given in Table 1.

Crystallographic data for this structure has been deposited with the Cambridge Crystallographic Data Centre as supplementary data no. CCDC 288837. Copies of the data may be obtained free of charge upon request from the director, Cambridge Crystallographic Data Centre, 12 Union Road, Cambridge CB2 1EZ, UK. (Fax: +44-1223-336033. E-mail: deposit@ccdc.cam.ac.uk. Web site: http://www.ccdc.cam.ac.uk.

Micro-Raman Measurements. Micro-Raman spectra were obtained with a Jobin Yvon LABRAM integrated Raman spectroscopy system at 180° backscatter with an MSPlan 100× objective, mounted in an Olympus 40XB microscope. The powder samples were mounted on a fused silica substrate. Either 633 nm helium−neon laser light or 785 nm Ti:sapphire laser light was focused onto the sample with an MSPlan 100× microscope objective, providing an illuminated spot. The spot size is approximately 2 μm in diameter and 8−10 μm in thickness (Z direction). The scattered light was detected through a 250 μm slit, yielding a detected resolution better than 0.5 nm or 4 cm^{-1}. The power of the unfiltered laser is about 250 mW. Neutral density filters were used to decrease the laser power until it was determined that the laser was not damaging the sample. The laser power used depended on the sample and the wavelength. The collection of Raman spectra of silver salts must be approached with caution. We have found here and in related work that silver salts can be extremely sensitive to laser irradiation, which can cause damage that may not be visible. For this work, we found that an excitation wavelength of 785 nm did less damage to the sample than an excitation wavelength of 633 nm. Unfortunately, the notch filter available for the LabRam does not allow data collection much below 100 cm^{-1}. Data were necessarily collected using the He−Ne laser, with an excitation wavelength of 633 nm, because a Horiba SuperNotch filter is available for that wavelength, allowing collection of data to about 77 cm^{-1}. Data collected below 100 cm^{-1} with the SuperNotch filter were still noisy, however.

Computational Methods. All DFT calculations were done using *Gaussian 98*, revision A.9,[14a] or *Jaguar*, version 5.0.[14b] The B3LYP method[9] was generally used. When used with the LANL2DZ effective core potential (ECP) basis set,[15a−c] the B3LYP method has been shown to provide good structures and vibrational frequencies for complexes of Group Ib coinage metals (Cu, Ag, Au).[15d] Other calculations used B3LYP or BLYP with the DZVP (double-ζ valence + polarization) all-electron basis set[16] rather than an ECP basis. B3LYP/DZVP calculations have been shown to be useful for calculations of many silver complexes.[17] In *Gaussian 98*, Atoms in Molecules (AIM)[10] calculations do not function correctly with ECP-type bases, so an all-electron basis set is required when using AIM. A few semiempirical AM1 calculations[18] were done, using *Mopac 2000* as a test of the AM1 parametrization for silver using the AM1-d method[18c] where d orbital functions are present on heavy elements. The hope was that this method might prove useful for computations on large silver-containing clusters. Vibrational frequency calculations (B3LYP/DZVP) that were used to compute

(12) The *SORTAV* program is based on the method of Blessing; see Blessing, R. H. *Acta Crystallogr., Sect. A* **1995**, *51*, 33.
(13) Sheldrick, G. M. *SHELXTL*: *Structure Analysis Program*, version 6.10; Bruker Analytical X-ray systems: Madison, WI, 2000.
(14) Frisch, M. J.; Trucks, G. W.; Schlegel, H. B.; Scuseria, G. E.; Robb, M. A.; Cheeseman, J. R.; Zakrzewski, V. G.; Montgomery, J. A., Jr.; Stratmann, R. E.; Burant, J. C.; Dapprich, S.; Millam, J. M.; Daniels, A. D.; Kudin, K. N.; Strain, M. C.; Farkas, O.; Tomasi, J.; Barone, V.; Cossi, M.; Cammi, R.; Mennucci, B.; Pomelli, C.; Adamo, C.; Clifford, S.; Ochterski, J.; Petersson, G. A.; Ayala, P. Y.; Cui, Q.; Morokuma, K.; Malick, D. K.; Rabuck, A. D.; Raghavachari, K.; Foresman, J. B.; Cioslowski, J.; Ortiz, J. V.; Stefanov, B. B.; Liu, G.; Liashenko, A.; Piskorz, P.; Komaromi, I.; Gomperts, R.; Martin, R. L.; Fox, D. J.; Keith, T.; Al-Laham, M. A.; Peng, C. Y.; Nanayakkara, A.; Gonzalez, C.; Challacombe, M.; Gill, P. M. W.; Johnson, B. G.; Chen, W.; Wong, M. W.; Andres, J. L.; Head-Gordon, M.; Replogle, E. S.; Pople, J. A. *Gaussian 98*, revision A.9; Gaussian, Inc.: Pittsburgh, PA, 1998.
(15) (a) Hay, P. J.; Wadt, W. R. *J. Chem. Phys.* **1985**, *82*, 270. (b) Wadt, W. R.; Hay, P. J. *J. Chem. Phys.* **1985**, *82*, 284. (c) Hay, P. J.; Wadt, W. R. *J. Chem. Phys.* **1985**, *82*, 299. (d) Legge, F. S.; Nyberg, G. L.; Peel, J. B. *J. Phys. Chem. A* **2001**, *105*, 7905.
(16) Godbout, N.; Salahub, D. R.; Andzelm, J.; Wimmer, E. *Can. J. Chem.* **1992**, *70*, 560.

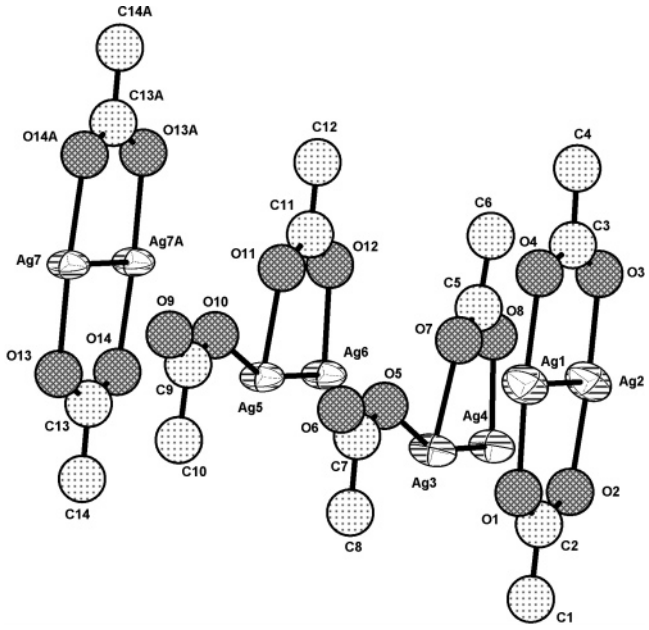

Figure 2. Crystallographic atomic labeling scheme and structure of silver acetate complex. Probability ellipsoids are at the 50% level for Ag atoms. C and O atoms were left isotropic during refinement. H atoms are omitted for clarity.

Raman spectra revealed no imaginary frequencies for the optimized complexes $Ag_2(O_2CCH_3)_2$ in C_{2h} symmetry and for $[Ag_2(O_2CCH_3)_2]_3$ in C_i symmetry.

Results and Discussion

Solid-State Structure of Silver Acetate. Figure 2 illustrates the atomic labeling scheme and structure of the silver acetate complex. Probability ellipsoids are at the 50% level for Ag atoms. X-ray crystallographic results reveal that the asymmetric unit contains seven silver acetate molecules. However, the molecular structure of the repeating subunit in this structure is a symmetric dimer. There is a close interaction (2.794(4)−2.809(3) Å) between the two silver atoms. These distances are all shorter than the analogous interaction in silver trifluoroacetate[3b] (2.967(3) Å). Selected Ag−Ag and Ag−O bond lengths are listed in Table 2. The Ag−Ag bonding pattern in unit cell packing is illustrated in Figure 3.

Notably, the published solid-state ^{109}Ag NMR spectrum[19] of silver acetate (but not other simple silver carboxylates) shows two peaks at 401.2 and 382.7 ppm relative to $AgNO_3$, with a relative peak height of approximately 2:1. So far, it is not clear how this result can be reconciled with our X-ray crystallographic structure with seven unique Ag ions in the asymmetric unit (however, computational work is planned using NMR calculations on the X-ray structure and using periodic boundary condition methods).

Comparison of Theoretical and Experimental $Ag_2(O_2C_2H_3)_2$ Structures. For many silver carboxylates, the repeating unit in the crystalline solid is a $Ag_2(carboxylate)_2$ dimer, sometimes depicted as an eight-membered ring with the carboxylates bridging the metal ions. Of interest to this study is that the silver ions at the 1 and 5 positions of the "eight-membered ring" are in proximity, typically 2.7−3.0 Å, similar to the Ag−Ag distance of 2.889 Å in metallic silver. This suggests that a bonding interaction may exist between the two silver ions. If so, the dimer should be properly considered as two fused five-membered rings, a question that can be directly evaluated using quantum mechanical modeling.

As a model for the solid-state environment of the silver acetate dimer, the model oligomer structure $[Ag_2(O_2C_2H_3)_2]_3$ was optimized (Figure 4). This model does not address nonbonded stacking interactions between the continuous ribbons, but it does at least test the ability of theoretical methods to reproduce the directly bonded interdimer Ag−O interactions. The heavy atom skeleton of the $[Ag_2(O_2C_2H_3)_2]_3$ structure optimizes to C_i symmetry; however, a quite flat potential-energy surface with respect to methyl group rotations makes this scarcely lower in energy than C_1. Among the three dimers in this structure, the two dimers at either end are distorted by edge effects. Focusing on the central dimer, the Ag−Ag distance is 2.92 Å at the B3LYP/LANL2DZ level and 3.07 Å at the B3LYP/DZVP level. Although B3LYP/DZVP has been documented as giving generally good results for a variety of silver complexes (see ref 20 and references therein for discussion), it somewhat overestimates the Ag−Ag distance compared to experimental values. With the DZVP basis set, the BLYP method finds a Ag−Ag distance of 3.01 Å, closer to experimental values but still not as good as the LANL2DZ ECP basis. This is consistent with previous findings[5] that aurophilic and argentophilic interactions are significantly relativistic in nature, as the ECP takes relativistic effects into account. Notably, calculations at the AM1-d level gave severe out-of-plane distortions of the ligands, thereby collapsing the structure.

The structure of an isolated $Ag_2(O_2C_2H_3)_2$ subunit (Figure 5) was also computed at several theoretical levels (Table 3), and it is interesting to note that its structure is not very different from that of the central dimer subunit in the supramolecular $[Ag_2(O_2C_2H_3)_2]_3$ structure. This suggests that the isolated $Ag_2(O_2C_2H_3)_2$ unit is a reasonable model system. The semiempirical AM1-d calculation gives a reasonable

(17) (a) Shoeib, T.; Milburn, R. K.; Koyanagi, G. K.; Lavrov, V. V.; Bohme, D. K.; Siu, K. W. M.; Hopkinson, A. C. *Int. J. Mass Spectrom.* **2000**, *201*, 87. (b) Shoeib, T.; El Aribi, H.; Siu, K. W. M.; Hopkinson, A. C. *J. Phys. Chem. A* **2001**, *105*, 710. (c) Shoeib, T.; Rodriquez, C. F.; Siu, K. W. M.; Hopkinson, A. C. *Phys. Chem. Chem. Phys.* **2001**, *3*, 853. (d) Shoeib, T.; Hopkinson, A. C.; Siu, K. W. M. *J. Phys. Chem. B* **2001**, *105*, 12399. (e) El Aribi, H.; Shoieb, T.; Rodriquez, C. F.; Hopkinson, A. C.; Siu, K. W. M. *J. Phys. Chem. A* **2002**, *106*, 2098. (f) Shoeib, T.; Siu, K. W. M.; Hopkinson, A. C. *J. Phys. Chem. A* **2002**, *106*, 6121. (g) Clarke, A. J.; Ingleson, M. J.; Kociok-Kohn, G.; Mahon, M. F.; Patmore, N. J.; Rourke, J. P.; Ruggiero, G. D.; Weller, A. S. *J. Am. Chem. Soc.* **2004**, *126*, 1503. (h) Unpublished work from our own laboratories has shown that B3LYP/DZVP gives good results for reproducing or predicting many experimental phenomena related to silver complexes, although Ag−Ag bonding distances are usually somewhat overestimated.

(18) Stewart, J. J. P. *MOPAC 2000*; Fujitsu Limited: Tokyo, 1999. (b) Dewar, M. J. S.; Zoebisch, E. G.; Healy, E. F.; Stewart, J. J. P. *J. Am. Chem. Soc.* **1985**, *107*, 3902. (c) Voityuk, A. A. AM1-d method for silver. *Abstracts of Papers*, 227th National Meeting of the American Chemical Society, Anaheim, CA, March 28−April 1, 2004; American Chemical Society: Washington, DC, 2004; COMP-072.

(19) Merwin, L. H.; Sebald, A. *J. Magn. Reson.* **1992**, *97*, 628.

(20) Bringley, J. F.; Rajeswaran, M.; Olson, L. P.; Liebert, N. *J. Solid State Chem.* **2005**, *178*, 3074.

Table 2. Selected Bond Lengths (Å) for Silver Acetate

Ag(1)−Ag(2)	2.809(3)	Ag(3)−Ag(4)	2.806(3)	Ag(7)−O(14)#3	2.199(12)
Ag(5)−Ag(6)	2.804(3)	Ag(7)−Ag(7)#3	2.794(4)	Ag(1)−O(2)#1	2.407(19)
Ag(1)−O(1)	2.162(17)	Ag(1)−O(4)	2.225(16)	Ag(2)−O(4)#2	2.412(15)
Ag(2)−O(3)	2.162(16)	Ag(2)−O(2)	2.208(19)	Ag(3)−O(5)	2.386(14)
Ag(3)−O(6)#2	2.206(14)	Ag(3)−O(7)	2.231(14)	Ag(4)−O(7)#2	2.430(13)
Ag(4)−O(8)	2.180(14)	Ag(4)−O(5)#2	2.225(14)	Ag(5)−O(10)	2.408(14)
Ag(5)−O(9)#2	2.164(13)	Ag(5)−O(11)	2.187(12)	Ag(6)−O(11)#2	2.407(12)
Ag(6)−O(12)	2.191(12)	Ag(6)−O(10)#2	2.254(14)	Ag(7)−O(14)#1	2.442(11)
Ag(7)−O(13)	2.191(12)				

result for this structure, even though it failed for the $[Ag_2(O_2C_2H_3)_2]_3$ structure.

AIM Results for $Ag_2(O_2C_2H_3)_2$. The AIM methodology of Bader and co-workers was used to evaluate whether Ag(I)−Ag(I) bonding is present or absent in $Ag_2(O_2C_2H_3)_2$. The specific AIM/B3LYP/DZVP methods used, as well as background information on the reliability of the B3LYP/DZVP method for silver complexes, have recently been described elsewhere.[20] For the $Ag_2(O_2C_2H_3)_2$ structure, AIM finds (in addition to the expected C−H, C−C, C−O, and O−Ag bond critical points, or BCPs) no ring critical point defining an eight-membered ring; rather, there are two ring critical points, defining two fused five-membered rings. AIM also finds a BCP between the two silver ions (Figure 5). Despite B3LYP/DZVP somewhat exaggerating the metal−metal separation, AIM finds a Ag(I)−Ag(I) bond, i.e., an argentophilic interaction. The AIM calculation was repeated for the larger $[Ag_2(O_2C_2H_3)_2]_3$ structure, and the findings regarding intradimer Ag−Ag bonding were the same. This calculation found that the interdimer Ag−Ag interaction (3.64 Å) is nonbonding, though there are Ag−O bonds (2.39−2.43 Å) between dimers.

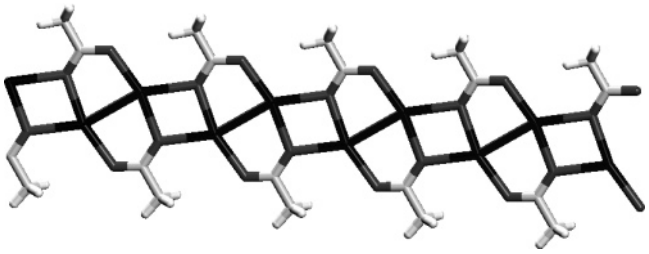

Figure 3. Ag−Ag bonding pattern in silver acetate packing diagram.

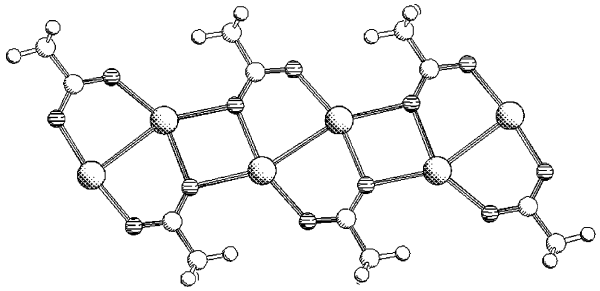

Figure 4. Model $[Ag_2(O_2C_2H_3)_2]_3$ structure, optimized at the B3LYP/DZVP level of theory. The flanking (i.e., first and third) subunits are distorted as a result of edge effects. Figures 4, 5, and 9 were prepared using *SCHAKAL*.[24a]

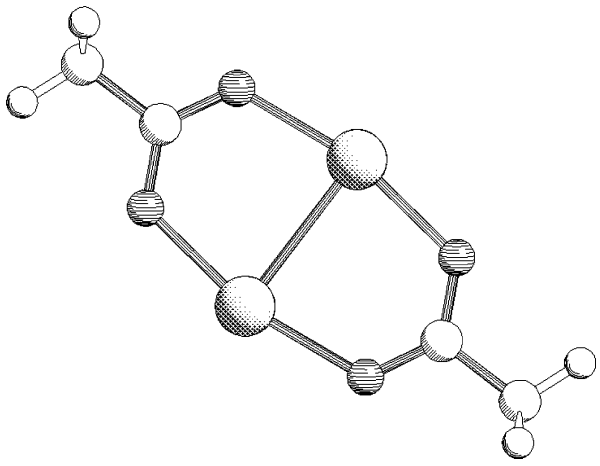

Figure 5. Computed structure of $Ag_2(O_2C_2H_3)_2$.

Table 3. Selected Ag−Ag and Ag−O Distances, Determined at Various Levels of Theory, for $Ag_2(OAc)_2$

method	Ag−Ag distance (Å)	Ag−O distance (Å)
B3LYP/LANL2DZ	2.82	2.16
B3LYP/LANL2DZ[a]	2.92	2.21−2.27
B3LYP/DZVP	2.92	2.20
B3LYP/DZVP[a]	3.06	2.25−2.31
BLYP/DZVP	2.88	2.21
BLYP/DZVP[a]	3.01	2.26−2.33
AM1-d	2.87	2.13

[a] Central unit of $[Ag_2(O_2CH_3)_2]_3$.

Molecular Orbitals of $Ag_2(O_2C_2H_3)_2$. The d^{10}−d^{10} closed-shell attraction between metal centers has been analyzed in considerable detail theoretically.[5c,d,g,h,21] The conclusions of these studies are generally to credit some combination of correlation, relativistic, and excitation effects (varying as a function of the metals and/or ligands) for the attraction, whereas classical bonding and orbital hybridization effects are largely discounted. Nonetheless, the frontier orbitals (the LUMO in particular) are relevant for the present study because they may explain silver acetate behavior following single-electron reduction.

The B3LYP/DZVP HOMO and LUMO of the isolated dimer $Ag_2(O_2C_2H_3)_2$ structure are shown in Figure 6. The HOMO is Ag−O antibonding and Ag−Ag antibonding, a_u symmetry, −7.185 eV. The LUMO, on the other hand, is Ag−O antibonding but Ag−Ag bonding, a_g symmetry, −1.480 eV.

The HOMO and LUMO of the $[Ag_2(O_2C_2H_3)_2]_3$ structure are shown in Figure 7. Here, the HOMO (−6.965 eV) resembles that of the isolated dimer, but in an all-antibonding combination between dimers.

Note that (at least for this size oligomer) the HOMO coefficients are reasonably balanced across all three dimer units. The $[Ag_2(O_2C_2H_3)_2]_3$ LUMO (−1.653 eV), again, is like that of the corresponding isolated dimer. However, unlike the HOMO, the LUMO is localized on the central dimer.

(21) (a) Pyykkö, P.; Mendizabal, F. *Inorg. Chem.* **1998**, *37*, 3018. (b) Pyykkö, P.; Tamm, T. *Organometallics* **1998**, *17*, 4842 and references therein. (c) O'Grady, E.; Kaltsoyannis, N. *Chem. Phys. Phys. Chem.* **2004**, *6*, 680 and references therein.

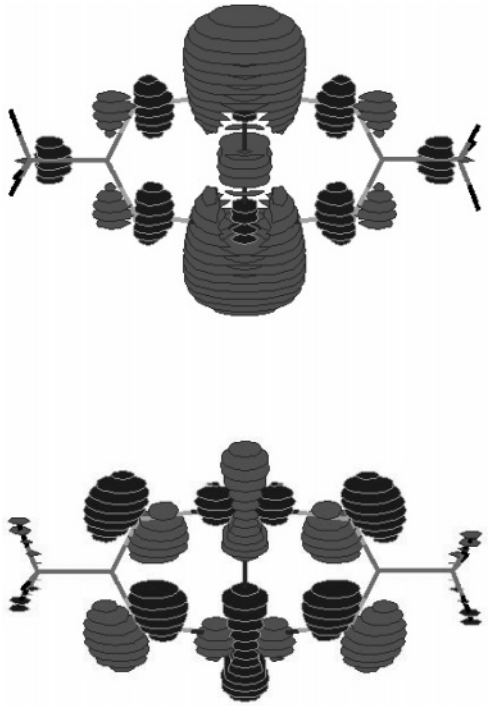

Figure 6. Molecular orbitals #79 (LUMO, top) and #78 (HOMO, bottom) of $Ag_2(O_2C_2H_3)_2$. Figure prepared using *MOLDEN*.[24b]

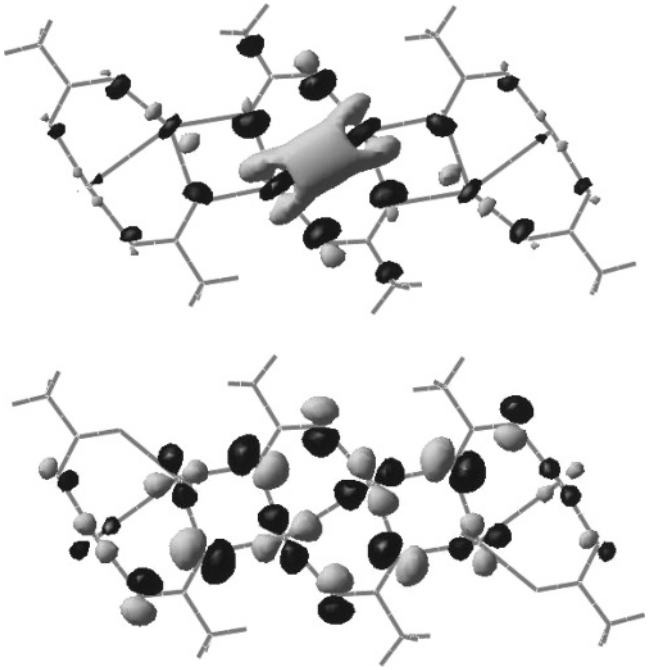

Figure 7. Molecular orbitals #235 (LUMO, top) and #234 (HOMO, bottom) of $[Ag_2(O_2C_2H_3)_2]_3$. Figure prepared using *MAESTRO*.[24c]

There is, as expected, some narrowing of the computed band gap when comparing $Ag_2(O_2C_2H_3)_2$ to $[Ag_2(O_2C_2H_3)_2]_3$; however, the gap is still large enough to be consistent with silver acetate being a colorless compound.

Raman Spectra of Silver Acetate. Previous studies have demonstrated strong Raman scattering associated with Au(I)−Au(I) and Ag(I)−Ag(I) bonds. In some cases, it is possible to correlate the bond-stretching force constants with metal−metal separation.[22a] Notably, silver acetate (like other simple silver carboxylates) comprises dimers that are not isolated inasmuch as they are bonded to their neighbors by Ag−O interactions. This continuously bonded network may serve to couple vibrational modes across individual dimers in the chain, so Ag−Ag stretching vibrations, in this case, may not fall in line with published correlations (whereas for solid-state structures comprising relatively isolated M_2L_2 molecules,[22] the M−M distance vs frequency relationship might be expected to hold true).[23]

Figure 8 shows the experimental Raman spectra for silver acetate that were collected with 785 and 633 nm laser excitation. Excitation with a 785 nm laser is preferable for silver acetate because of the slight degradation of the sample during data collection with 633 nm excitation. However, the ROI lies below 200 cm^{-1}. Silver acetate exhibits some fluorescence at this excitation wavelength. The inset shows (uncorrected) data collected above 400 cm^{-1} at both excitation wavelengths, demonstrating that all the bands observed when the compound is stimulated with 785 nm are also observed at 633 nm excitation. Therefore, the data collected with 633 nm excitation are acceptable.

B3LYP/DZVP vibrational frequency results (50−400 cm^{-1} range) for the $[Ag_2(O_2C_2H_3)_2]_3$ model structure are shown in Figure 9. Most significant are Raman-active Ag−Ag stretching frequencies of 81 and 85 cm^{-1}. This seems similar to the 81 cm^{-1} peak found experimentally, most clearly seen at 785 nm excitation (only seen as a shoulder at 633 nm excitation).

The overall Raman experimental and computational results support the AIM finding of a Ag−Ag bond in silver acetate.

Computed Geometry and Electronic Structure of $[Ag_2(O_2C_2H_3)_2]^{-\bullet}$. It has been proposed[2] that the interaction between pairs of silver ions in crystalline silver carboxylates may lead to enhanced latent image formation upon reduction, e.g., by developer. It seems possible that the addition of a single electron to the dimeric subunit could generate $(Ag_2)^{+\bullet}$, a partially reduced silver cluster that is the smallest possible stable latent image center in the Gurney-Mott latent image theory.[7] The reasons why $(Ag_2)^{+\bullet}$ is considered the smallest stable latent image center in photography have to do with recombination processes in a silver halide crystal. Lone silver atoms carry the electron in a photogenerated electron/hole pair in silver halide, but such pairs may collapse unless the lone silver atom encounters a Ag(I) ion to form $(Ag_2)^{+\bullet}$, which stabilizes the photoelectron against recombination. Such recombination issues might not apply to lone silver atoms that might form in silver carboxylates, but the results presented so far make $(Ag_2)^{+\bullet}$ formation in silver carboxylates seem entirely plausible. Inasmuch as Ag(I)−Ag(I) bonds are present even prior to adding electrons, the metal−metal bonding nature of the LUMO should serve only to reinforce this tendency.

To simulate a single-electron reduction process, we computed the geometry and electronic structure of the reduced complex $[Ag_2(O_2C_2H_3)_2]^{-\bullet}$ at the UB3LYP/DZVP

(22) Perreault, D.; Drouin, M.; Machel, A.; Miskowski, V. M.; Schaefer, W.; Harvery, P. D. *Inorg. Chem.* **1992**, *31*, 695. (b) Che, C.-M.; Lai, S.-W. *Coord. Chem. Rev.* **2005**, *249*, 1296. (c) Phillips, D. L.; Che, C.-M.; Leung, K. H.; Mao, Z.; Tse, M.-C. *Coord. Chem. Rev.* **2005**, *249*, 1476.

(23) Work is in progress to compare Raman frequencies with Ag−Ag distances in other silver carboxylates.

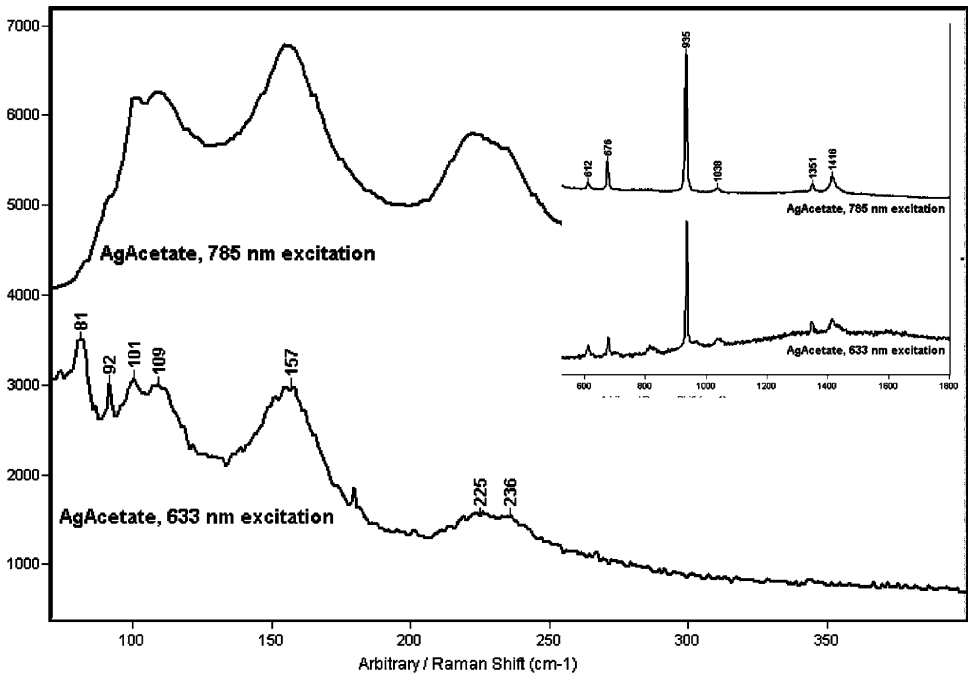

Figure 8. Raman spectra of silver acetate at 633 nm (top) and 785 nm (bottom) excitation (inset is data collected above 400 cm^{-1}); the data are not corrected.

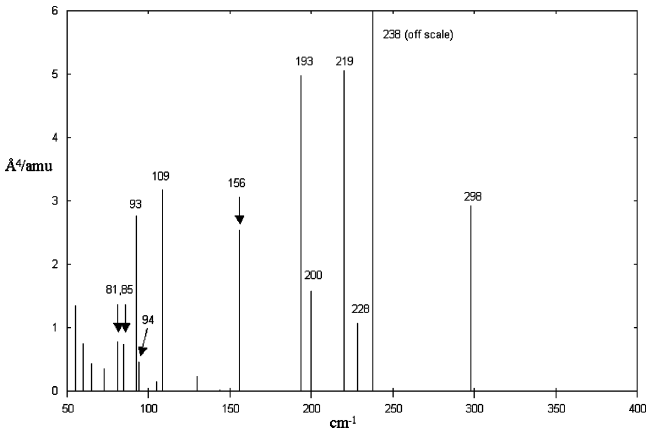

Figure 9. B3LYP/DZVP computed Raman scattering frequencies (cm^{-1}) and intensities ($Å^4$/amu) over the range 50−400 cm^{-1} for the $[Ag_2(O_2C_2H_3)_2]_3$ structure of Figure 4. Selected frequencies are labeled, with arrows denoting significant involvement of Ag−Ag stretching (especially 81 and 85 cm^{-1}, relatively "pure" stretching frequencies).

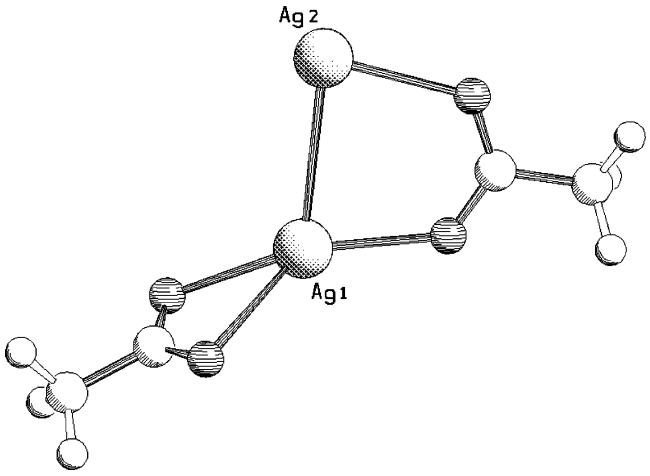

Figure 10. UB3LYP/DZVP structure of the radical anion of $Ag_2(O_2C_2H_3)_2$. Mulliken charge and spin densities are consistent with a $(Ag_2)^+$ ion complexed to two carboxylates; however, the bulk of the positive charge resides on Ag1, and the bulk of the spin density resides on Ag2.

level, using the structure of the neutral complex as the starting point. Following geometry optimization, the radical anion is rearranged significantly from the structure of the neutral complex, Figure 10.

The structure, atomic charges, and spin density within this radical anion are consistent with $(Ag_2)^{+\bullet}$ complexed to two acetate anions. Despite the metal−metal bonding nature of the SOMO (i.e., the LUMO of the neutral dimer) and the expectation that much of the coulomb repulsion between the two metal centers should be relieved by the presence of this electron, the Ag−Ag distance (3.05 Å) is not much different from the distance found in the neutral complex. It is interesting to note that optical excitation of a Ag(I)−Ag(I) bonded species is predicted[25] to result in a significant shortening of the Ag−Ag distance. The presence of a Ag−Ag bond in the radical anion was proven by an AIM calculation, which finds a BCP between these silver nuclei and ring critical points corresponding to two spiro-fused rings with a silver ion at the shared corner. Table 4 provides a comparison of some computed properties of $Ag_2(O_2C_2H_3)_2$ in its neutral- and radical-anion forms.

Whereas an isolated $(Ag_2)^{+\bullet}$ cluster is symmetric, in so much as charge and unpaired spin density are shared evenly between the silver nuclei, that is not the case for the $[Ag_2(O_2C_2H_3)_2]^{-\bullet}$ structure computed here. Rather, the $(Ag_2)^{+\bullet}$ cluster in $[Ag_2(O_2C_2H_3)_2]^{-\bullet}$ resembles a Ag(I) center bonded to a Ag(0) center. The Ag(I) center is complexed to both carboxylates, whereas the other silver, which has an

(24) (a) *SCHAKAL*: www.krist.uni-freiburg.de/ki/Mitarbeiter/Keller/schakal.html. (b) *MOLDEN*: Schaftenaar, G.; Noordik, J. H. *J. Comput.-Aided Mol. Des.* **2000**, *24*, 123. (c) *MAESTRO interface*; Schrodinger, LLC: Portland, OR, 2005.

(25) Rawashdeh-Omary, M. A.; Omary, M. A.; Patterson, H. H.; Fackler, J. P. *J. Am. Chem. Soc.* **2001**, *123*, 11237.

Table 4. Comparison of Computed Properties of $Ag_2(O_2C_2H_3)_2$ in Neutral and Radical Anion Forms[a]

property	$Ag_2(O_2C_2H_3)_2$	$Ag_2(O_2C_2H_3)_2$ radical anion
B3LYP/DZVP SCF energy	−10856.134289 hartrees	−10856.167748 hartrees
Mulliken charges on silver	+0.579, +0.579	−0.113 (Ag2), +0.475 (Ag1)
UB3LYP atomic spin density on silver	not applicable	0.893 (Ag2), 0.044 (Ag1)
AIM density Laplacian ($\nabla^2\rho(r)$) value for the Ag−Ag bond critical point	+0.0824	+0.0602

[a] Note that the atoms in molecules (AIM) atomic charges were qualitatively similar to the Mulliken charges for the radical anion species; however, the AIM atomic charge-fitting algorithm for the neutral species failed in *Gaussian 98*. Note that the $\nabla^2\rho(r)$ value is >0 in both cases; this is characteristic of a closed-shell interaction.

atomic charge (−0.113) and unpaired spin density (0.893) consistent with Ag(0), is bonded to only one oxygen. Despite caveats related to differences in Ag−Ag electron distribution in isolated vs complexed clusters of (partially) reduced silver, these quantum mechanical results support the hypothesis that single-electron reduction of a $Ag_2(O_2CR)_2$ complex might result in the formation of the latent image center $(Ag_2)^{+\bullet}$.

Conclusions

The single-crystal X-ray crystal structure of silver acetate is reported for the first time. This is a model for larger silver carboxylates in PTG materials and as precursors of silver nanoparticles. Quantum mechanical DFT methods were used to evaluate the electronic structure of the silver carboxylate dimer, $Ag_2(O_2C_2H_3)_2$, and the larger species $[Ag_2(O_2C_2H_3)_2]_3$. The AIM/B3LYP/DZVP results unambiguously support the existence of the Ag(I)−Ag(I) bond in this complex. Vibrational frequency calculations on $[Ag_2(O_2C_2H_3)_2]_3$ indicate Raman-active Ag−Ag stretching frequencies of 81 and 85 cm^{-1}, comparable to the Raman scattering peak we observe at ∼81 cm^{-1}. The structure of the radical anion $(Ag_2(OAc)_2)^{-\bullet}$ was used as a model for the single-electron reduction of $Ag_2(OAc)_2$ by the developer. The AIM/UB3LYP/DZVP analysis of the optimized structure of $(Ag_2(OAc)_2)^{-\bullet}$ is consistent with the predicted minimal stable latent image center $(Ag_2)^{+\bullet}$ complexed with two carboxylate ions. This supports previous proposals regarding the image formation ability of Ag behenate, if it were to capture an electron from the developer.

Acknowledgment. The authors thank Dr. Victor Young and William Brennessel from the University of Minnesota for their help with several trials of data collection and the structure determination of silver acetate. Additional thanks are due to Dr. Young for helpful discussions regarding the structure and constructive feedback regarding this paper.

CM052657V